

See discussions, stats, and author profiles for this publication at: <https://www.researchgate.net/publication/7416134>

Infrared Spectrum and Structural Assignment of the Water Trimer Anion †

ARTICLE in THE JOURNAL OF PHYSICAL CHEMISTRY A · JANUARY 2006

Impact Factor: 2.69 · DOI: 10.1021/jp053769c · Source: PubMed

CITATIONS

27

READS

31

5 AUTHORS, INCLUDING:



Nathan I Hammer

University of Mississippi

87 PUBLICATIONS 2,149 CITATIONS

SEE PROFILE



Joseph R Roscioli

Aerodyne Research, Inc.

45 PUBLICATIONS 1,445 CITATIONS

SEE PROFILE



Evgeniy M. Myshakin

AECOM / National Energy Technology Labora...

49 PUBLICATIONS 1,153 CITATIONS

SEE PROFILE



Kenneth D Jordan

University of Pittsburgh

372 PUBLICATIONS 13,830 CITATIONS

SEE PROFILE

Infrared Spectrum and Structural Assignment of the Water Trimer Anion[†]N. I. Hammer,[‡] J. R. Roscioli,[‡] M. A. Johnson,^{*,‡} E. M. Myshakin,[§] and K. D. Jordan^{*,§}*Sterling Chemistry Laboratory, Yale University, P.O. Box 208107, New Haven, Connecticut 06520, and Department of Chemistry and Center for Molecular and Materials Simulations, University of Pittsburgh, Pittsburgh, Pennsylvania 15260**Received: July 8, 2005; In Final Form: August 5, 2005*

The bending vibrational spectrum of the perdeutero isotopomer of the water trimer anion has been measured and compared with spectra calculated using the MP2, CCSD, and Becke3LYP electronic structure methods. Due to its low electron binding energy (≈ 150 meV), only the OD bending region of the IR spectrum of $(\text{D}_2\text{O})_3^-$ is accessible experimentally, with electron ejection dominating at higher photon energies. The calculated spectrum of the isomer having three water molecules arranged in a chain agrees best with the experimental spectrum. In the chain isomer, the excess electron is bound to the terminal water monomer with two dangling OH groups. This is consistent with the electron binding mechanism established previously for the $(\text{H}_2\text{O})_n^-$ ($n = 2, 4-6$) anions.

Introduction

Negatively charged water clusters, $(\text{H}_2\text{O})_n^-$, have enjoyed a storied history.¹⁻¹⁴ $(\text{H}_2\text{O})_n^-$ ions were first detected mass spectroscopically in 1984,¹⁵ and the photoelectron spectra of these clusters were reported by Bowen and co-workers in 1990.¹ While the $n = 2, 6, 7$ and ≥ 11 $(\text{H}_2\text{O})_n^-$ clusters can be made in abundance, the $n = 3-5$ and $8-10$ $(\text{H}_2\text{O})_n^-$ ions are much less abundant in the mass spectral distributions.^{1,5,6,9,15,16} Indeed, until recently, the $n = 4$ ion had not been observed.¹⁷ The mass spectra and photoelectron spectra alone are insufficient for establishing the geometrical structures of the anionic clusters. The development of experimental techniques for obtaining the vibrational spectra of $(\text{H}_2\text{O})_n^-$ clusters,¹⁸⁻²² discussed below, has greatly advanced our understanding of their preferred methods of electron accommodation.

Water clusters do not possess low-lying valence molecular orbitals to accommodate an excess electron, and the observed anions (at least for the size range considered here) can be viewed as being electrostatically bound.^{6,23-25} It is known that molecules or clusters with dipole moments greater than about 2.5 D are generally able to form stable dipole-bound anions in which the excess electron is primarily bound in the long-range dipole field.^{23,26,27} The most stable forms of the neutral $n = 2, 6$, and 7 clusters have sizable ($\mu > 2.7$ D) dipole moments²⁸⁻³⁰ whereas the global minimum structures of the $n = 3-5$, and 8 clusters have zero or near zero dipole moments. For example, although the global minimum of $(\text{H}_2\text{O})_3$ is calculated to have a dipole moment of 1.07 D, upon averaging over the low-frequency motion involving flipping of the free OH groups, the dipole averages to zero.³⁰ This suggests that the high intensities of the $n = 2, 6, 7$ anions in the $(\text{H}_2\text{O})_n^-$ mass spectrum is a consequence of direct electron capture, $(\text{H}_2\text{O})_n + e^- \rightarrow (\text{H}_2\text{O})_n^-$, and that the absence or weak signals for the $n = 3-5$ and $8-10$ anions is a consequence of the absence of a direct capture

formation process for these clusters. Indeed, it has been established recently that the dominant form of $(\text{H}_2\text{O})_6^-$ results from electron capture by the book isomer of the neutral $(\text{H}_2\text{O})_6$ cluster.^{21,22} In the absence of a direct electron capture process, a $(\text{H}_2\text{O})_n^-$ anion can be formed via a growth process: i.e., via $(\text{H}_2\text{O})_{n-1}^- + \text{H}_2\text{O} \rightarrow (\text{H}_2\text{O})_n^-$. Argon-mediated addition of a water monomer to $(\text{H}_2\text{O})_3^-$ has been used to prepare the “missing” $(\text{H}_2\text{O})_4^-$ cluster.^{17,21}

The structure of the $(\text{H}_2\text{O})_2^-$ anion is well-established on the basis of theoretical studies.³¹⁻³³ Specifically, the dimer anion adopts a “linear” cis arrangement in contrast to the trans structure of the neutral dimer. Preference for the cis orientation in the anion is a consequence of the larger dipole moment and, hence, larger electron binding energy for this orientation.^{32,33}

Vibrational predissociation spectroscopy has proven especially valuable for elucidating the structures of the $(\text{H}_2\text{O})_n^-$ ($n = 4-6$) clusters. Specifically, by this means, it has been possible to establish that the observed $(\text{H}_2\text{O})_4^-$ ion has a ring structure and that the dominant forms of the $n = 5$ and 6 anions have fused-ring structures. For each of these anions the excess electron interacts primarily with one double-acceptor water molecule, positioned so that both of its hydrogen atoms are oriented in the direction of the excess electron.²¹ The importance of the double-acceptor site for binding the excess electron in the $n = 4-6$ clusters was first revealed in the theoretical study of Lee et al.³³

Although $(\text{H}_2\text{O})_3^-$ can be synthesized, its structure has remained a mystery. From photoelectron spectroscopy (PES), the vertical detachment energy (VDE) of $(\text{H}_2\text{O})_3^-$ has been determined to be about 150 meV (≈ 1200 cm⁻¹).³⁴ As a result of the low electron binding energy, the HOH bending (~ 1600 cm⁻¹) and OH and OD stretching (~ 3700 and ~ 2500 cm⁻¹, respectively) transitions lie in the electronic continuum, and electron ejection at these photon energies is so rapid that vibrational structure is not observed. The problem presented by electron detachment is less severe in the clusters with higher electron binding energies. For example, for $(\text{H}_2\text{O})_4^-$ and $(\text{H}_2\text{O})_5^-$, it was possible to obtain spectra in the OH and OD bending regions as well as in the OD stretch region; for the

[†] Part of the special issue “Jack Simons Festschrift”.

^{*} Address correspondence to either author. E-mail: jordan@pitt.edu (K.D.J.); mark.johnson@yale.edu (M.A.J.).

[‡] Yale University.

[§] University of Pittsburgh.

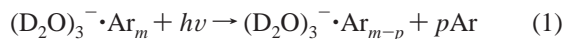
(H₂O)₆[−] cluster, it was also possible to obtain vibrational spectra in the OH stretching region of the spectrum. In the present study of the water trimer anion, we have been forced to focus on the OD bending region [of (D₂O)₃[−]], for which electron ejection is sufficiently slow to permit sharp vibrational structure.

It is now well-established that electron correlation effects can drastically impact the binding energies of dipole-bound anions.^{23,35–42} The main correlation contribution is a dispersion-type interaction between the excess electron and the electrons of the polar molecules comprising the cluster.^{23,36–39} In many cases, fourth- and higher-order correlation effects also make sizable contributions to the electron binding energies, requiring the use of the computationally demanding coupled-cluster methods.^{43,44} Moreover, the extended nature of the excess electron requires the use of large, flexible basis sets, making the theoretical description of dipole-bound anions by ab initio methods exceedingly challenging.

Most calculations of the vibrational spectra of (H₂O)_{*n*}[−] ions have employed the Becke3LYP^{45,46} density functional or MP2⁴⁷ methods. In general, the MP2 method tends to underestimate the electron binding energies of dipole-bound anions.¹⁴ In contrast, the Becke3LYP density functional method, when used with flexible basis sets, tends to considerably overbind the excess electron.¹⁴ This clearly reflects unphysical behavior on the part of the Becke3LYP method as it does not incorporate long-range dispersion interactions.¹⁴ Despite the limitations of the Becke3LYP and MP2 methods for describing the binding of the excess electron, both approaches have proven valuable in assigning the observed vibrational spectra of (H₂O)_{*n*}[−] ions.^{33,48–51} The (H₂O)₃[−] cluster is small enough that it is possible to optimize the geometries and to calculate the vibrational spectra at the CCSD level of theory, which should largely overcome the limitations of the Becke3LYP and MP2 methods for characterizing the weakly bound anions. In this work, the geometries of three isomers of (H₂O)₃[−] have been optimized and their vibrational spectra calculated at each of the MP2, CCSD, and Becke3LYP levels of theory.

Methodology

Experimental Details. The bending vibrational spectrum of (D₂O)₃[−] was obtained by employing the messenger technique,⁵² with Ar atoms as the messengers.⁵³ When vibrationally excited, energy redistribution in (D₂O)_{*n*}[−]·Ar_{*m*} clusters results in the loss of argon atoms such that



This method has recently been applied to (H₂O)_{*n*}[−]·Ar_{*m*} (*n* = 4–6).^{21,53} Here, (D₂O)₃[−]·Ar_{*m*} (*m* = 3, 6, and 11) ions were created by slow electron attachment to neutral water clusters solvated with argon, at a point in the expansion that collisions with water monomers were still possible. (D₂O)₃[−]·Ar_{*m*} ions, mass selected using a double-focusing, tandem time-of-flight mass spectrometer,^{54,55} were irradiated with the mid-IR output from a Nd:YAG pumped OPO/OPA (LaserVision) laser. The reported spectrum results from the addition of 23 individual scans, corrected for laser pulse energy changes over the scan range. Attempts to obtain infrared spectra in the HOH bending and OH and OD stretching regions resulted only in electron detachment and failed to yield vibrational structure.

Computational Details. Three isomeric forms of (H₂O)₃[−] were considered in the theoretical investigation. These isomers, depicted in Figure 1, consist of a C_{2v} symmetry structure with a double-acceptor water flanked by two single-donor monomers

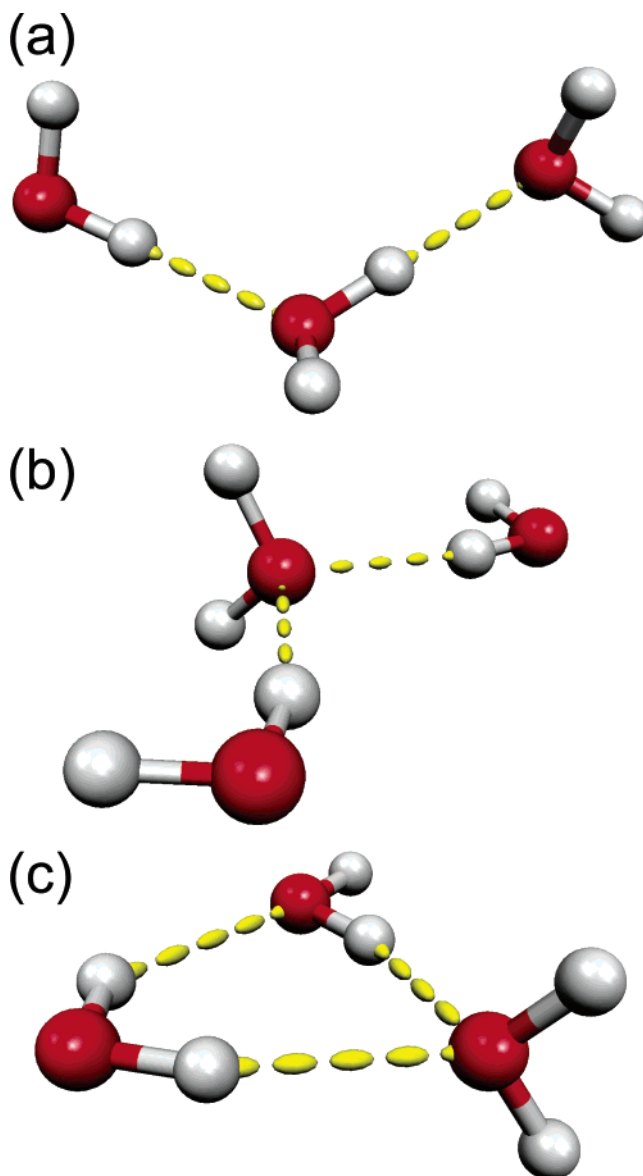


Figure 1. Optimized structures of the water trimer anion: (a) chain, (b) C_{2v}, and (c) cyclic.

(Figure 1b); a cyclic structure (Figure 1c) with double-acceptor, double-donor, and acceptor–donor water monomers; and a chain-like species with one donor (D), one acceptor (A), and one acceptor–donor (AD) water monomer (Figure 1a). Each of these isomers has a large ($\mu > 6$ D) dipole moment and is thus assured of having a dipole-bound anion.^{23,26,27} A fourth isomer of (H₂O)₃[−], with a cyclic structure with three DA monomers and the three free OH groups pointed in the same direction, was ruled out as it has a near zero vertical electron detachment energy that is much less than the experimental value.^{33,56} The geometries were optimized at the Becke3LYP, MP2, and CCSD levels of theory, and the vibrational spectra for the optimized structures were calculated in the harmonic approximation using each of the three theoretical methods. Single-point CCSD(T) calculations were carried out on the neutral and anionic species at the MP2-optimized geometries of the anions to obtain estimates of the VDEs.

The three (H₂O)₃[−] isomers considered here were previously reported in refs 33 and 51, where vibrational frequencies were reported only for the Becke3LYP and MP2 levels of theory, and only in the OH stretching region of the spectrum. Here, we report calculated spectra in the OD bend region and examine

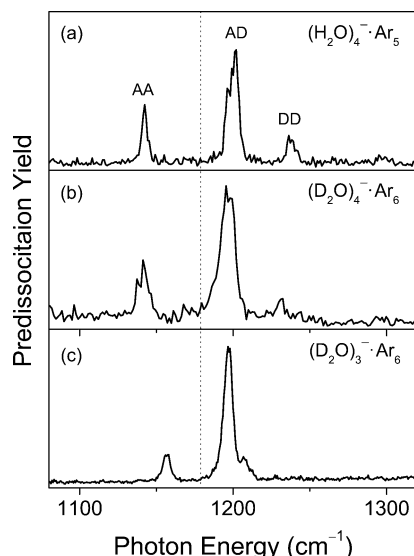


Figure 2. Vibrational predissociation spectra of (a) $(\text{H}_2\text{O})_4^-\cdot\text{Ar}_5$, (b) $(\text{D}_2\text{O})_4^-\cdot\text{Ar}_6$, and $(\text{D}_2\text{O})_3^-\cdot\text{Ar}_6$ in the HOH and DOD bending regions. The frequencies of $(\text{H}_2\text{O})_4^-\cdot\text{Ar}_5$ have been scaled by the ratio of the measured frequencies of the free water bends of D_2O and H_2O (1178/1595 cm^{-1}). The dotted lines indicate the locations of the bending frequencies of gas-phase H_2O (1595 cm^{-1}) and D_2O (1178 cm^{-1}). The labels AA, AD, and DD in (a) represent assignment of these spectral features in the tetramer anion to double-acceptor, single-acceptor/single-donor, and double-donor water molecules, respectively.

whether inclusion of high-order correlation effects changes in the calculated spectra.

The Becke3LYP calculations were carried out using a 6-311++G***(sp)* basis set,^{47,57} formed by adding to the standard 6-311++G** basis set diffuse *sp* functions with exponent 0.0105625 on oxygen atoms.^{33,49,50} Kim and co-workers have previously characterized several low-lying minima of the $(\text{H}_2\text{O})_n^-$, $n \leq 8$, clusters using this approach.^{33,49,50} The MP2, CCSD, and CCSD(T) calculations were carried out using the aug-cc-pVDZ(2s2p/2s) basis set, formed by augmenting the standard aug-cc-pVDZ basis set^{58,59} with two sets of diffuse *sp* functions on the O atoms and two diffuse *s* functions on the H atoms. The supplemental diffuse functions were taken from the work of Kim and co-workers.^{33,49–51} The Gaussian 03 program suite⁴⁷ was used for the calculations.

Results and Discussion

Infrared Spectra of the Water Trimer and Tetramer Anions. Figure 2 reports the experimental IR predissociation spectra of $(\text{D}_2\text{O})_3^-\cdot\text{Ar}_6$ and $(\text{D}_2\text{O})_4^-\cdot\text{Ar}_6$ from 1275 to 1350 cm^{-1} . For comparison, the corresponding spectrum of $(\text{H}_2\text{O})_4^-$ is reproduced from ref 21, with the frequencies being scaled by the ratio of the bending frequencies of D_2O and H_2O . It is important to point out that the IR predissociation spectra obtained for $(\text{D}_2\text{O})_3^-\cdot\text{Ar}_3$ and $(\text{D}_2\text{O})_3^-\cdot\text{Ar}_{11}$ are virtually identical to that shown in Figure 2c for $(\text{D}_2\text{O})_3^-\cdot\text{Ar}_6$.

The dotted lines in Figure 2 indicate the locations of the free bend vibration in an isolated water molecule (1595 and 1178 cm^{-1} , for H_2O and D_2O , respectively). In each spectrum there exists a transition that is *lower in energy* than this benchmark. This feature occurs at 1159 cm^{-1} in $(\text{D}_2\text{O})_3^-$ and at 1141 cm^{-1} in $(\text{D}_2\text{O})_4^-$. This growing red-shift continues with increasing number of water molecules (at least up to the hexamer) with a peak position of 1134 cm^{-1} in the hexamer anion.⁵³ This peak has been shown to be the spectral signature of a double-acceptor water molecule with two free OH groups that plays a major

TABLE 1: Relative Energies (kcal/mol) and Vertical Detachment Energies (meV) of Three Isomers of $(\text{H}_2\text{O})_3^-$ ^a

method	isomer		
	C_{2v}	cyclic	chain
B3LYP	1.86	0.46 ^b	0 ^b
MP2	2.24 ^c	0.29 ^b	0 ^c
CCSD//MP2 ^d	1.88 ^c	0.08 ^b	0 ^c
CCSD ^e	1.89	0.09	0
CCSD(T)//MP2 ^d	1.88 ^c	0	0.01 ^c
B3LYP + ZPE _{B3LYP}	1.53	0.74 ^b	0 ^b
MP2 + ZPE _{MP2}	2.00 ^c	0.55 ^b	0 ^c
CCSD ^d + cZPE _{MP2}	1.64 ^c	0.34 ^b	0
CCSD(T) ^d + ZPE _{MP2}	1.64 ^c	0.25	0
CCSD ^e + ZPE _{CCSD}	1.65	0.34	0
CCSD(T) ^d + ZPE _{CCSD}	1.65	0.24	0
VDE _{MP2}	145 ^c	110 ^b	114 ^c
VDE _{CCSD/MP2}	174 ^c	134	136 ^c
VDE _{CCSD}	170	129	132
VDE _{CCSD(T)/MP2}	187 ^c	145	146 ^c

^a The B3LYP calculations were performed using the 6-311++G***(sp)* basis set, and the MP2, CCSD, and CCSD(T) calculations were carried out using the aug-cc-pVDZ(2s2p/2s) basis set. ^b From ref 33. ^c From ref 51. ^d Calculated at the MP2 geometry. ^e Calculated at the CCSD geometry.

role in the binding of the excess electron.²¹ It is interesting that although the absolute red-shift of this feature from the free water bend is appreciably different for $(\text{H}_2\text{O})_4^-$ and $(\text{D}_2\text{O})_4^-$, the relative red-shift for the two isotopomers is identical.

The feature at 1198 cm^{-1} (20 cm^{-1} higher in energy than the free bend) in both $(\text{D}_2\text{O})_3^-$ (Figure 2c) and $(\text{D}_2\text{O})_4^-$ (Figure 2b) has been assigned to the bending vibration of a single hydrogen-bond acceptor, single hydrogen-bond donor (AD) water molecule in the latter case.²¹ Missing in Figure 2c, however, is a feature at 1220 cm^{-1} , which would have indicated the presence of a double hydrogen-bond donating (DD) water molecule. In its place is a weak transition at 1209 cm^{-1} , which was not observed in the infrared spectra of the $n = 4$ –6 clusters.

Comparison with Theory. Each of the three isomers of $(\text{H}_2\text{O})_3^-$ depicted in Figure 1 can be formed by adding a water molecule to the water dimer anion. Our calculations indicate that these addition reactions occur with no net barrier. At the highest level of theory considered (CCSD(T)//MP2 with ZPE corrections based on CCSD frequencies calculated at the CCSD geometries), the chain isomer (Figure 1a) is predicted to be most stable, followed by the cyclic (Figure 1c), 0.24 kcal/mol higher in energy, and then the C_{2v} structure (Figure 1b), which is calculated to be 1.65 kcal/mol less stable than the chain structure (Table 1). The C_{2v} structure is calculated to have a VDE of 187 meV, whereas the other two isomers are calculated to have VDEs of about 145 meV, close to the 150 meV experimental value of the VDE. Based on energetic considerations, both the chain and cyclic isomers of $(\text{H}_2\text{O})_3^-$ are viable candidates for the observed anion. Both of these isomers have the excess electron bound in the vicinity of a water molecule with two free OH groups, consistent with the presence of the strongly red-shifted bending vibration in the experimental spectrum.

Figure 3 compares the calculated (CCSD level, frequencies scaled by 0.975) vibrational spectra for the chain, cyclic, and C_{2v} isomers of $(\text{D}_2\text{O})_3^-$ with the experimental spectrum of $(\text{D}_2\text{O})_3^-\cdot\text{Ar}_6$. (The scale factor was chosen so as to bring the harmonic bending frequency calculated for D_2O into agreement with the experimental bending frequency.) The calculated spectrum of the cyclic isomer (Figure 3d) differs appreciably from the experimental spectrum (Figure 3a), whereas the calculated spectra of both the C_{2v} (Figure 3c) and chain (Figure 3b) isomers possess transitions close to those observed experi-

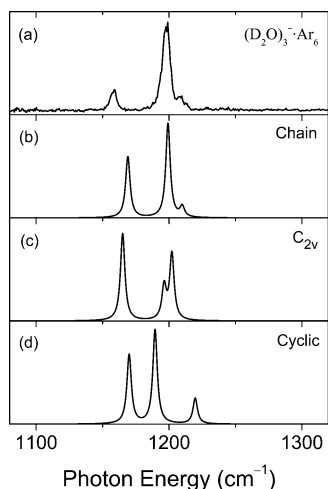


Figure 3. Comparison of the (a) experimental spectrum of $(\text{D}_2\text{O})_3^-\cdot\text{Ar}_6$ with the calculated vibrational spectra of three isomers of the water trimer anion: (b) chain, (c) C_{2v} , and (d) cyclic. The calculated spectra were obtained in the harmonic approximation using the CCSD/aug-cc-pVDZ(2s2p/2s) methods. The calculated frequencies were scaled by 0.975.

mentally. However, the relative peak positions and intensities for the calculated spectrum of the chain isomer are in better agreement with those measured experimentally. On the basis of the energetic considerations and on comparison of the calculated and measured vibrational spectra in the OD bending region, we conclude that the observed $(\text{D}_2\text{O})_3^-$ anion is most likely the chain isomer, depicted in Figure 1a. This assignment assumes that the attached Ar atoms do not appreciably alter the frequencies of the OD bending vibrations. This was checked by optimizing the geometry and calculating the vibrational spectrum of $(\text{D}_2\text{O})_3^-\cdot\text{Ar}_3$ using the Becke3LYP method. The resulting spectrum in the bending region is indeed nearly identical to that calculated for the bare $(\text{D}_2\text{O})_3^-$ cluster.

In the calculated spectrum of the chain isomer, the most red-shifted OD bending vibration is associated with the terminal acceptor monomer of the chain, and the intense bending vibration about 41 cm^{-1} to the blue of the low energy band is due to the in-phase combination of the D and AD bends. This is followed by a weak band, 8 cm^{-1} further to the blue, due to the out-of-phase combination of the D and AD bends.

Table 2 summarizes the calculated frequencies and intensities for the chain form of the $(\text{D}_2\text{O})_3^-$ anion at each of the three theoretical methods considered. The MP2 and CCSD methods give nearly the same splittings between the three bending vibrations (and close to those measured experimentally), whereas the Becke3LYP splittings are about 30% larger. There are also large differences between the intensities for the bending vibrations calculated using MP2 and CCSD methods and those calculated using the Becke3LYP method, with the former being significantly larger. None of the theoretical methods considered gives relative intensities of the three bending vibrations in good agreement with experiment. The reason for this is not clear.

Given the low intensity of $(\text{H}_2\text{O})_3^-$ in the mass spectrum of negatively charged water clusters, it appears likely that the observed trimer anions are formed by addition of a water monomer to the dimer anion, rather than via electron capture by the neutral trimer, which, under the conditions of the experiments, should be dominated by the global minimum cyclic species (with three acceptor–donor monomers). It was demonstrated previously that the dominant form of $(\text{H}_2\text{O})_4^-$ results from Ar-mediated addition of H_2O to $(\text{H}_2\text{O})_3^-$.¹⁷ It is not clear

TABLE 2: Calculated Harmonic Frequencies (cm^{-1}) and Intensities (km/mol) of the Chain Isomer of $(\text{D}_2\text{O})_3^-$ ^a

vibration ^b	CCSD		MP2		B3LYP	
	freq	int	freq	int	freq	int
OD stretch (D)	2853	200	2848	182	2825	98
OD stretch (AD)	2843	475	2837	469	2794	601
OD stretch (A)	2830	2530	2833	3337	2705	1130
OD stretch (A)	2712	3437	2704	6848	2622	225
OD stretch (D/AD)	2679	364	2630	429	2601	312
OD stretch (AD/D)	2646	7049	2590	8124	2541	463
DOD bend (D/AD)	1241	121	1223	113	1227	66
DOD bend (AD/D)	1230	1097	1211	899	1211	230
DOD bend (A)	1199	712	1181	778	1161	159
OD wag (AD)	523	410	542	375	582	128
OD wag (D)	485	441	501	333	538	105
DOD rock (AD/D)	277	45	288	32	306	15
DOD rock (AD/D)	238	203	248	186	262	39
D- -O IM stretch	216	171	224	167	235	35
DOD rock(A)	177	383	183	749	210	4
DOD wag (A)	169	1777	176	1437	184	804
OD wag (AD/A)	152	411	159	426	167	127
D- -O IM stretch	142	347	147	372	156	82
OD wag (D)	74	68	74	41	94	12
DOD rock (A)	45	381	48	337	50	116
D- -O IM rock	26	44	28	44	32	20
ZPE (kcal/mol)	32.55		32.42		32.18	

^a The MP2 and CCSD results were obtained with the aug-cc-pVDZ(2s2p/2s) basis set and the Becke3LYP results with the 6-311++G**(sp) basis set. The frequencies reported in the table are unscaled. ^b AD, acceptor–donor water monomer; D, donor water monomer; A, acceptor water monomer.

why addition of a water monomer to $(\text{H}_2\text{O})_2^-$ favors formation of the chain isomer over the cyclic isomer, but it is possible that approach of a water monomer to $(\text{H}_2\text{O})_2^-$ with orientations that favor formation of the cyclic structure (Figure 1c) tends to lead to electron detachment.

Conclusions

The water trimer anion has eluded vibrational analysis until now because of its low electron binding energy. In the present work this problem was overcome by measuring the vibrational spectrum of $(\text{D}_2\text{O})_3^-$ in the OD bending region. The lower frequency of the $(\text{D}_2\text{O})_3^-$ bending vibrations as compared to those of $(\text{H}_2\text{O})_3^-$ suppresses electron autoionization, enabling the detection of sharp vibrational structure. The geometries of three possible structural isomers were optimized, and the corresponding vibrational frequencies were calculated at the CCSD/aug-cc-pVDZ(2s2p/2s) level of theory. The best overall agreement between theory and experiment is found for the chain isomer in which the electron is bound in the vicinity of the terminal single-acceptor water molecule with two dangling OH groups. This isomer is also predicted to be the most stable form of the anion and to have a vertical detachment energy close to that observed experimentally. This assignment is consistent with those recently made for the $n = 4$ –6 anions, for which the excess electron is also bound in the vicinity of a water monomer with two dangling OH groups, although for these larger clusters the monomer with the two dangling OH groups resides in a double-acceptor site, and isomers with fused rings dominate. The redshift of the bending frequency associated with the AA or A water monomer increases as one progresses from $(\text{D}_2\text{O})_3^-$ to $(\text{D}_2\text{O})_6^-$. The VDEs also increase along this sequence, which suggests that the redshift grows with increasing localization of the excess electron.

Acknowledgment. M.A.J. and K.D.J. thank the Department of Energy (Grant DR-FG02-00ER15066) for support of this

research. The calculations were carried out on computers in the University of Pittsburgh's Center of Molecular and Materials Simulations, which were funded by grants from IBM and NSF.

References and Notes

- (1) Coe, J. V.; Lee, G. H.; Eaton, J. G.; Arnold, S. T.; Sarkas, H. W.; Bowen, K. H.; Ludewigt, C.; Harberland, H.; Worsnop, D. R. *J. Chem. Phys.* **1990**, *92*, 3980.
- (2) Posey, L. A.; Johnson, M. A. *J. Chem. Phys.* **1988**, *89*, 4807.
- (3) Campagnola, P. J.; Cyr, D. M.; Johnson, M. A. *Chem. Phys. Lett.* **1991**, *181*, 206.
- (4) Posey, L. A.; Campagnola, P. J.; Johnson, M. A.; Lee, G. H.; Eaton, J. G.; Bowen, K. H. *J. Chem. Phys.* **1989**, *91*, 6536.
- (5) Lee, G. H.; Arnold, S. T.; Eaton, J. G.; Sarkas, H. W.; Bowen, K. H.; Ludewigt, C.; Harberland, H. Z. *Phys. D: At., Mol. Clusters* **1991**, *20*, 9.
- (6) Desfrancois, C.; Khelifa, N.; Lisfi, A.; Schermann, J. P.; Eaton, J. G.; Bowen, K. H. *J. Chem. Phys.* **1991**, *95*, 7760.
- (7) Tachikawa, D. H.; Lund, A.; Ogasawara, M. *Can. J. Chem.* **1993**, *71*, 118.
- (8) Misaizu, F.; Kondow, T.; Kuchitsu, K. *Chem. Phys. Lett.* **1997**, *178*, 369.
- (9) Maeyama, T.; Tsumura, T.; Fujii, A.; Mikami, N. *Chem. Phys. Lett.* **1997**, *264*, 292.
- (10) Bailey, C. G.; Kim, J.; Johnson, M. A. *J. Phys. Chem.* **1996**, *100*, 16782.
- (11) Ayotte, P.; Bailey, C. G.; Kim, J.; Johnson, M. A. *J. Chem. Phys.* **1998**, *108*, 444.
- (12) Kelley, J. A.; Weddle, G. H.; Robertson, W. H.; Johnson, M. A. *J. Chem. Phys.* **2002**, *116*, 1201.
- (13) Weber, J. M.; Leber, E.; Ruf, M.-W.; Hotop, H. *Eur. Phys. J. D* **1999**, *7*, 587.
- (14) Ayotte, P.; Weddle, G. H.; Bailey, C. G.; Johnson, M. A.; Vila, F.; Jordan, K. D. *J. Chem. Phys.* **1999**, *110*, 6268.
- (15) Harberland, H.; Langosch, H.; Schindler, H.-G.; Worsnop, D. R. *J. Phys. Chem.* **1984**, *88*, 3903.
- (16) Kim, J.; Becker, I.; Cheshnovsky, O.; Johnson, M. A. *Chem. Phys. Lett.* **1998**, *297*, 90.
- (17) Shin, J.-W.; Hammer, N. I.; Headrick, J. N.; Johnson, M. A. *Chem. Phys. Lett.* **2004**, *399*, 349.
- (18) Verlet, J. R. R.; Bragg, A. E.; Kammrath, A.; Cheshnovsky, O.; Neumark, D. N. *Science* **2005**, *307*, 93.
- (19) Paik, D. H.; Lee, I.-R.; Yang, D.-S.; Baskin, J. S.; Zewail, A. H. *Science* **2004**, *306*, 672.
- (20) Lu, Q.-B.; Baskin, J. S.; Zewail, A. H. *J. Phys. Chem. B* **2004**, *108*, 10509.
- (21) Hammer, N. I.; Shin, J.-W.; Headrick, J. M.; Diken, E. G.; Roscioli, G. R.; Weddle, G. H.; Johnson, M. A. *Science* **2004**, *306*, 675.
- (22) Diken, E. G.; Robertson, W. H.; Johnson, M. A. *J. Phys. Chem. A* **2004**, *108*, 64.
- (23) Wang, F.; Jordan, K. D. *Annu. Rev. Phys. Chem.* **2003**, *54*, 367.
- (24) Compton, R. N.; Hammer, N. I. In *Advances in Gas-Phase Ion Chemistry*; Adams, N. G., Ed.; JAI: Greenwich, 2001; Vol. 4, p 257.
- (25) Simons, J.; Skurski, P. In *Theoretical Prospects of Negative Ions*; Kalcher, J., Ed.; Research Signpost: Trivandrum, 2002; p 117.
- (26) Jordan, K. D. *Acc. Chem. Res.* **1979**, *12*, 36.
- (27) Simons, J.; Jordan, K. D. *Chem. Rev.* **1987**, *87*, 535.
- (28) Lee, H. M.; Suh, S. B.; Lee, J. Y.; Tarakeshwar, P.; Kim, K. S. *J. Chem. Phys.* **2000**, *112*, 9759.
- (29) Dyke, T. R.; Mack, K. M.; Muentner, J. S. *J. Chem. Phys.* **1977**, *66*, 498.
- (30) Gregory, J. K.; Clary, D. C.; Liu, K.; Brown, M. G.; Saykally, R. G. *Science* **1997**, *275*, 814.
- (31) Chipman, D. M. *J. Phys. Chem.* **1979**, *83*, 1657.
- (32) Chen, H.-Y.; Sheu, W.-S. *J. Chem. Phys.* **1999**, *110*, 9032.
- (33) Lee, H. M.; Lee, S.; Kim, K. S. *J. Chem. Phys.* **2003**, *119*, 187.
- (34) Kim, J.; Becker, I.; Cheshnovsky, O.; Johnson, M. A. *Chem. Phys. Lett.* **1998**, *297*, 90.
- (35) Gutowski, M.; Skurski, P.; Boldyrev, A. I.; Simons, J.; Jordan, K. D. *Phys. Rev. A* **1996**, *54*, 1906.
- (36) Gutowski, M.; Jordan, K. D.; Skurski, P. *J. Phys. Chem. A* **1998**, *102*, 2624.
- (37) Yokoyama, K.; Leach, G. W.; Kim, J. B.; Lineberger, W. C.; Boldyrev, A. I.; Gutowski, M. *J. Chem. Phys.* **1996**, *105*, 10706.
- (38) Gutowski, M.; Skurski, P. *Recent Res. Dev. Phys. Chem.* **1999**, *3*, 245.
- (39) Gutowski, M.; Skurski, P. *Chem. Phys. Lett.* **1999**, *300*, 331.
- (40) Adamowicz, L. *J. Chem. Phys.* **1989**, *91*, 7787.
- (41) Adamowicz, L.; McCullough, E. A. *J. Phys. Chem.* **1984**, *88*, 2045.
- (42) Desfrancois, C.; Periquet, V.; Carles, S.; Schermann, J. P.; Smith, D. M. A.; Adamowicz, L. *J. Chem. Phys.* **1999**, *110*, 4309.
- (43) Pople, J. A.; Head-Gordon, M.; Raghavachari, K. *J. Chem. Phys.* **1987**, *87*, 5968.
- (44) Peterson, K. A.; Gutowski, M. *J. Chem. Phys.* **2002**, *116*, 3297.
- (45) Becke, A. D. *J. Chem. Phys.* **1993**, *98*, 5648.
- (46) Lee, C.; Yang, W.; Parr, R. G. *Phys. Rev. B* **1998**, *37*, 785.
- (47) Frisch, M. J.; Trucks, G. W.; Schlegel, H. B.; Scuseria, G. E.; Robb, M. A.; Cheeseman, J. R.; Montgomery, J. A., Jr.; Vreven, T.; Kudin, K. N.; Burant, J. C.; Millam, J. M.; Iyengar, S. S.; Tomasi, J.; Barone, V.; Mennucci, B.; Cossi, M.; Scalmani, G.; Rega, N.; Petersson, G. A.; Nakatsuji, H.; Hada, M.; Ehara, M.; Toyota, K.; Fukuda, R.; Hasegawa, J.; Ishida, M.; Nakajima, T.; Honda, Y.; Kitao, O.; Nakai, H.; Klene, M.; Li, X.; Knox, J. E.; Hratchian, H. P.; Cross, J. B.; Bakken, V.; Adamo, C.; Jaramillo, J.; Gomperts, R.; Stratmann, R. E.; Yazyev, O.; Austin, A. J.; Cammi, R.; Pomelli, C.; Ochterski, J. W.; Ayala, P. Y.; Morokuma, K.; Voth, G. A.; Salvador, P.; Dannenberg, J. J.; Zakrzewski, V. G.; Dapprich, S.; Daniels, A. D.; Strain, M. C.; Farkas, O.; Malick, D. K.; Rabuck, A. D.; Raghavachari, K.; Foresman, J. B.; Ortiz, J. V.; Cui, Q.; Baboul, A. G.; Clifford, S.; Cioslowski, J.; Stefanov, B. B.; Liu, G.; Liashenko, A.; Piskorz, P.; Komaromi, I.; Martin, R. L.; Fox, D. J.; Keith, T.; Al-Laham, M. A.; Peng, C. Y.; Nanayakkara, A.; Challacombe, M.; Gill, P. M. W.; Johnson, B.; Chen, W.; Wong, M. W.; Gonzalez, C.; Pople, J. A. *Gaussian 03*; Gaussian, Inc.: Wallingford, CT, 2004.
- (48) Lee, H. M.; Lee, S.; Kim, K. S. *J. Chem. Phys.* **2003**, *119*, 7685.
- (49) Lee, H. M.; Kim, K. S. *J. Chem. Phys.* **2002**, *117*, 706.
- (50) Lee, H. M.; Suh, S. B.; Kim, K. S. *J. Chem. Phys.* **2003**, *118*, 9981.
- (51) Kim, J.; Suh, S. B.; Kim, K. S. *J. Chem. Phys.* **1999**, *111*, 10077.
- (52) Kumura, M.; Yeh, L.; Myers, J. D.; Lee, Y. T. *J. Chem. Phys.* **1986**, *85*, 2328.
- (53) Hammer, N. I.; Roscioli, R. J.; Johnson, M. A. *J. Phys. Chem. A* **2005**, *109*, 7896–7901.
- (54) Johnson, M. A.; Lineberger, W. C. In *Techniques for the Study of Ion–Molecule Reactions*; Farrar, J. J. M., Saunders, W. H., Eds.; Wiley: New York, 1988; p 591.
- (55) Posey, L. A.; Deluca, M. J.; Johnson, M. A. *Chem. Phys. Lett.* **1986**, *131*, 170.
- (56) Alfonso, D.; Jordan, K. D. *J. Chem. Phys.* **2002**, *116*, 3612.
- (57) Frisch, M. J.; Pople, J. A.; Binkley, J. S. *J. Chem. Phys.* **1984**, *80*, 3265.
- (58) Kendall, R. A.; Dunning, T. H., Jr.; Harrison, J. G. *J. Chem. Phys.* **1992**, *96*, 6796.
- (59) Woon, D. E.; Dunning, T. H., Jr. *J. Chem. Phys.* **1993**, *98*, 1358.